Thermal Engineering of the Cryogenic Beam Position Monitors for the EIC Hadron Storage Ring

F Micolon, J Bellon, V Chiechi, D M Gassner, C Hetzel, D Holmes, R Hulsart, V Ptitsyn, M Sangroula, S Verdu-Andres

BNL, Upton, New York, USA

Email: fmicolon@bnl.gov

Abstract. The Electron Ion Collider (EIC) Hadron Storage Ring (HSR) will reuse most of the existing superconducting magnets from the RHIC storage ring. However, the existing stripline beam position monitors (BPM) used for RHIC will not be compatible with the planned EIC hadron beam parameters that include higher intensity, shorter bunches, and some operational scenarios with large radial offsets of the beam in the vacuum chamber. To address these challenges, the existing RHIC stripline BPMs will be decommissioned, and a new BPM design using button pick-ups integrated in a new vacuum interconnect/bellows assembly will be installed adjacent to the decommissioned BPMs.
A dedicated analysis of the new BPM housing and button pick-up design has been conducted to assess the thermal effects caused by heat conduction, beam induced resistive wall heating and the RF heating from the BPM signal propagation through the cryogenic cables. This paper reports on the thermal design and analysis results to quantify the heat transfer and temperature distribution that can be expected on the new HSR cryogenic BPM.

1. Introduction

Featuring shorter particle bunches than RHIC [1] and large radial offsets for certain beam energies [2], the EIC hadron beams would produce an excessive voltage on the existing RHIC stripline BPMs. This would lead to high heating of the BPM module and its cryogenic signal cables [3]. Indeed, operational experience with the RHIC stripline BPMs has shown that their signal cables were already operating close to their limits [4]. To address these challenges, the existing RHIC stripline BPMs will be decommissioned and shielded, and a new BPM design using button pick-ups will be installed adjacent to the current BPMs [5].

A thermal analysis of the new arc BPM housing, button pick-up and cable has been conducted to assess the effects caused by beam induced heating and signal attenuation through the coaxial cables for several operational scenarios. We aim to share the strategy, the main findings, and conclusions of this engineering analysis in this paper.

2. System design and integration

A new HSR interconnect module has been designed to include the BPM button system as well as the RF fingers used to ensure electrical continuity between adjacent magnet beamline (Fig. 1). In this design, the BPM pickups are mounted at a 30° angle relative to the horizontal plane to avoid excessive heating when the beam is offset transversely [2]. The 316L BPM pick-ups will be copper plated to reduce heating by beam wall image current resistive heating. They will also be amorphous carbon coated to limit the secondary electron yield (SEY) and avoid generating additional electron cloud.

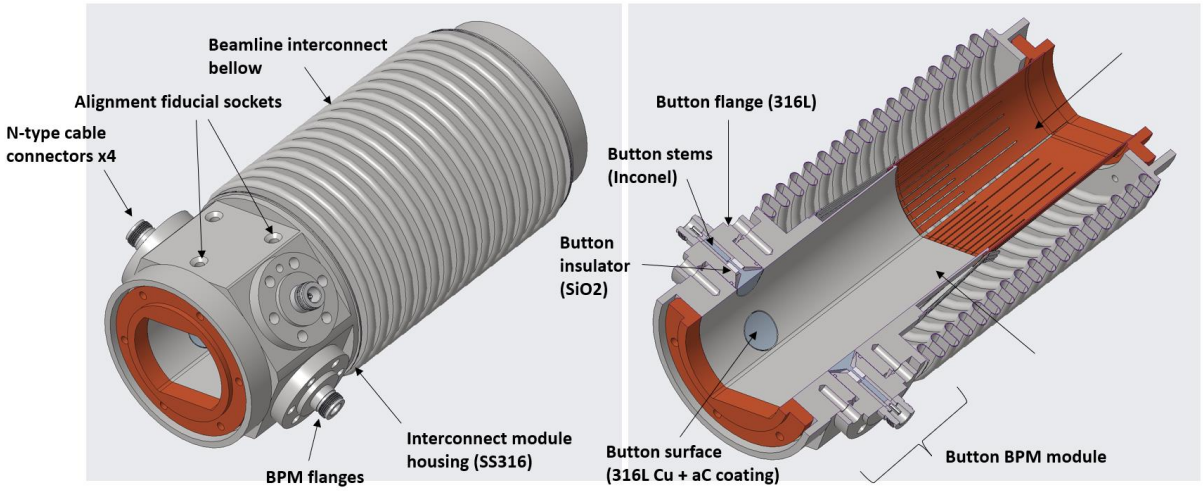

Figure 1. HSR BPM interconnect module layout

This interconnect module layout will be welded to the adjacent superconducting magnets in the HSR interconnect (Fig 2). The alignment of the BPM center to the adjacent quadrupole magnet will be crucial and alignment fiducials are included to enable this fine alignment.

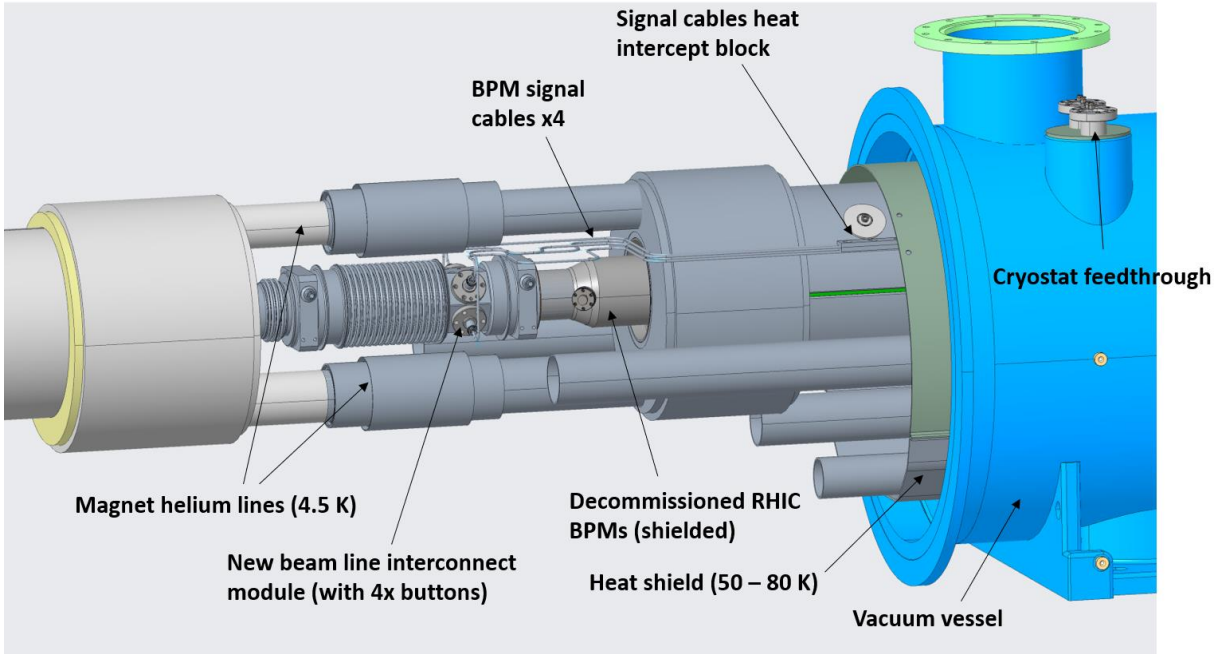

Figure 2. Integration of the interconnect module in the HSR

The BPM signal coaxial cables will connect to the cryogenically cooled interconnect module and will be routed along the magnet helium vessel to exit the vacuum vessel through the cryostat feedthrough. To limit the heat conducted from the cryostat feedthrough to the magnet, a heat intercept module will be placed on the cable path and will be connected to the heat shield by thermal straps.

3. Cable heat conduction and placement of the heat intercept

By bridging the cryostat feedthrough, held around 293 K by tunnel air convection, to the 4.5 K helium cooled magnet, the cryogenic cables will produce a heat leak to the cryogenic systems.

The heat conduction can be estimated with the thermal conductivity cryogenic integrals and the coaxial cable materials and dimensions from Table 1, see Fig 4.

Table 1. Dimensions and materials of some cryogenic coaxial used in relevant particle colliders.

Material	RHIC	LHC (from [8])	EIC – 0.141”	EIC – 0.090”
Outer conductor	304L (Ø 3.58 / 3.07 mm)	304L (Ø 3.58 / 2.97 mm) Cu RRR30 plating (0.10 mm Thick)	304L (Ø 3.58 / 3.07 mm) Cu RRR30 plating (0.08 mm Thick)	304L (Ø1.78 /2.29 mm) Cu RRR30 (0.025 mm Thick)
Dielectric	Tefzel (Ø 3.07 /0.81 mm)	Low density $Si0_2$ (Ø 0.94 mm/2.87 mm)	Low density $Si0_2$ (Ø3.07 mm/ 1.09 mm)	Low density $Si0_2$ (Ø 1.78 mm/ 0.64 mm)
Inner conductor	Cu RRR100 (Ø 0.81mm)	304L (Ø 0.86 mm) Cu RRR100 plating (Thick 0.04 mm)	Cu RRR100 (Ø 1.09mm)	Cu RRR100 (Ø 0.64.mm)

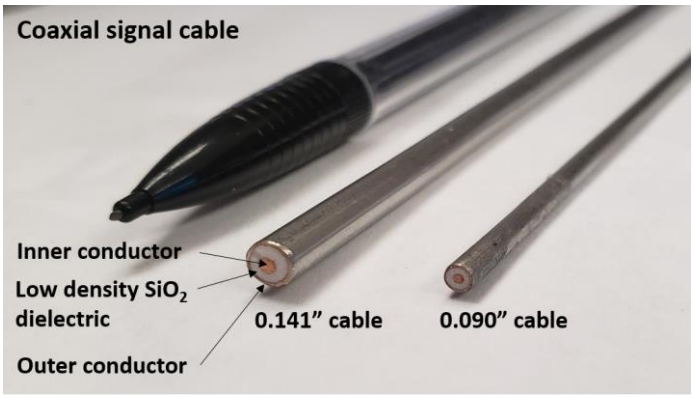

Figure 3. Cross section of sample SiO_2 coaxial signal cables

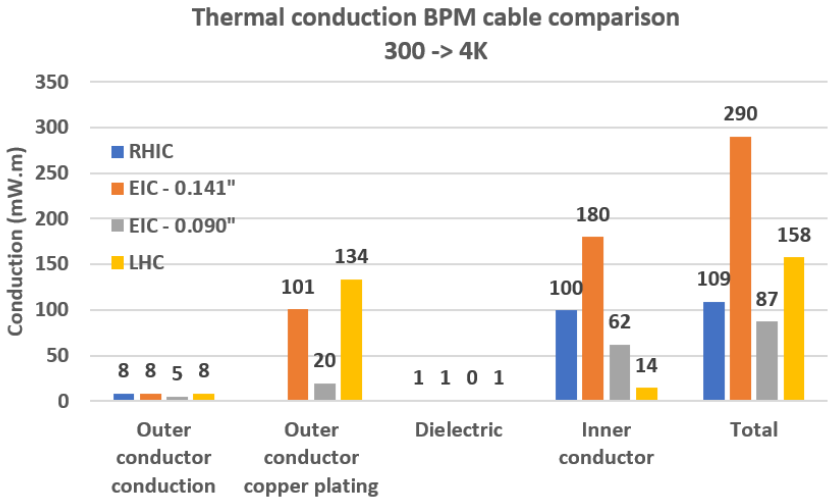

Figure 4. Comparison of the 300 – 4 K conductivity for selected BPM cables

In EIC, the magnet heat shield (50 – 80 K) can be used as a heat sink to mitigate this heat leak as was done for RHIC [6]. To place this heat intercept efficiently along the BPM cable, we have aimed to minimize the cryoplant cooling load. The RHIC cryoplant is considered to work with a Carnot efficiency around 20% [7] which gives the equivalent cryoplant loads displayed in Table 2.

Table 2. Cryoplant load for He at different temperature

Cryogenic cooling temperature (K)	80	50	4.5
Cryoplant power load (W/W)	13	25	321

We have aimed to find the optimal location of the heat intercept to minimize this cryoplant cooling power, assuming a 1.3 m cable length (Fig. 5).

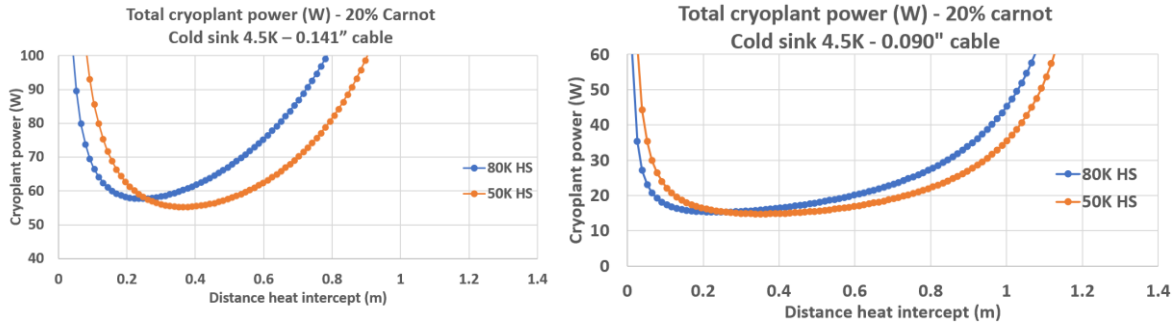

Figure 5. Cryoplant cooling load for different heat intercept location for a (left) Ø 0.141" (3.58 mm) (right) Ø 0.090" (2.29 mm) - 1.3 m long cable

For both the 0.141" and 0.090" cables, the optimal heat intercept placement, minimizing the cooling load from the cryogenic plant is between 0.2 – 0.4 m from the warm tunnel feedthrough (Fig 2).

4. Heat intercept design for coaxial cables

The heat intercept needs to be an effective heat sink while avoiding damage to the cable. The coaxial cables are delicate, with a fine outer jacket (see Fig 3) and any significant distortion of the dielectric can lead to undesired signal reflection within the cable. Brazing the cable to a heat intercept, although efficient, would be a labor-intensive operation and would also make a cable replacement operation more complex. Therefore, a solution with a bolted soft pure aluminum heat block was designed (Fig 6).

Pure aluminum has superior thermal conductivity properties while being able to yield and comply to the cable outer diameter. A finite element analysis with non-linear plastic material was made for a heat intercept groove of 9/64", slightly smaller than the nominal 0.141" cable (Fig 6). The required pressing force was adjusted to obtain a sufficient pressure at the interface while keeping the cable outer jacket yield at a minimum in the worst allowable tolerance (for both groove and cable).

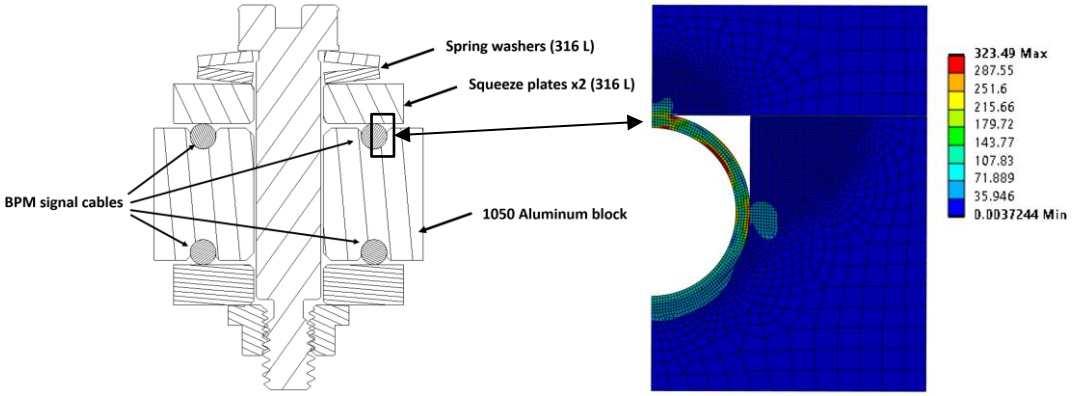

Figure 6. (Left) Cross section of planned BPM heat intercept block design (Right) analysis of the Von-Mises stress in the cable outer jacket

To limit the maximum force applied to the cable during assembly, and the associated coaxial cable distortion, a design with spring washers was engineered to limit the maximum force applied to a known value.

5. Evaluation of the cable RF heating

The propagation of an RF BPM signal along the coaxial signal cable will produce heat by resistive and dielectric losses. The cable heating will be conducted away mostly along the center and the outer conductor. The dielectric longitudinal conduction is marginal due to its low thermal conductivity.

5.1. Resistive heating

Given the intrinsically high frequency of the signal, image of a very short bunch of relativistic particles, the RF signal will propagate along a limited skin depth of the cable conductors.

So the cable resistance will be [8]: $R(T) = \frac{\Delta x.\sqrt{f.\rho_{i,e}(T)}}{r_{i,e}}$

And the resistive power dissipated will be: $P_{res}(T) = \frac{\Delta x.\sqrt{f.\rho_{i,e}(T)}}{r_{i,e}}.\int i^2.dt$

With

- $f\ [Hz]$ - signal reference frequency
- $\rho_{i,e}(T)\ [\Omega.m]$ - resistivity for the inner or outer conductor
- $r_{i,e}\ [m]$ - conductor radius for the inner or outer conductor
- Δx [m] – The length of cable considered

5.2. Dielectric heating

The power dissipated by dielectric loss will be:

$$P_{dielectric} = P_{RF}.\left(1 - 10^{\frac{-\alpha.\Delta x}{10}}\right) = f_b.Z_c.\int i^2 dt\,.\left(1 - 10^{\frac{-\alpha.\Delta x}{10}}\right)$$

With

- $\alpha\ [\frac{dB}{m}]$ - cable dielectric loss
- $f_b\ [Hz]$ - bunch revolution frequency
- $Z_c[\Omega]$ - characteristic impedance of the output port.

5.3. Cable conduction

The heat generated by resistive and dielectric losses will be conducted away through the cable to the cold end. The local temperature elevation will then be a function of the cable thermal conductivity.

$$P_{conduction} = -k(T).S_{i,e}.\frac{\Delta T}{\Delta x}$$

With

- $k(T)$ [W/m.K] is the conductor material thermal conductivity
- $S_{i,e}$ [m^2] the cross section of the inner or outer conductor
- $\frac{\Delta T}{\Delta x}$ [K/m] the temperature gradient along the cable

5.4. Summary – heat equation

The temperature of the cable will follow the heat conservation equation:

$$P_{resisitve} + P_{dielectric} + P_{conduction} = 0$$

$$\frac{\Delta x.\sqrt{f.\rho_{i,e}(T)}}{r_{i,e}}.\int i^2 dt + f_b.Z_c.\int i^2 dt\,.\left(1 - 10^{\frac{-\alpha.\Delta x}{10}}\right) - k(T).2\pi\, r_{i,e}.\frac{\Delta T}{\Delta x} = 0 \quad - \quad \text{Eq. (1)}$$

Since the cable temperature is not constant, the cable heating is evaluated along its length with a numerical model. A comparison was made with published data from the LHC cables [8] and showed a good agreement both on dissipated power and cable temperature [9].

6. RF heating of coaxial cables

A model of the cable alone was developed to evaluate the signal cable expected temperature and attenuation profile for different RF power. The cold side of the cable was fixed at 4.5 K while the hot side was fixed at 293 K. The 0.1 m long heat intercept at 80 K is located 0.35 m from the cable warm end (Fig. 3). The dimensions used can be found in Table 1. We have varied the signal RF power by varying the BPM signal peak voltage. The system matched impedance considered is 50 Ω and the average signal RF frequency was chosen as 1 GHz [9].

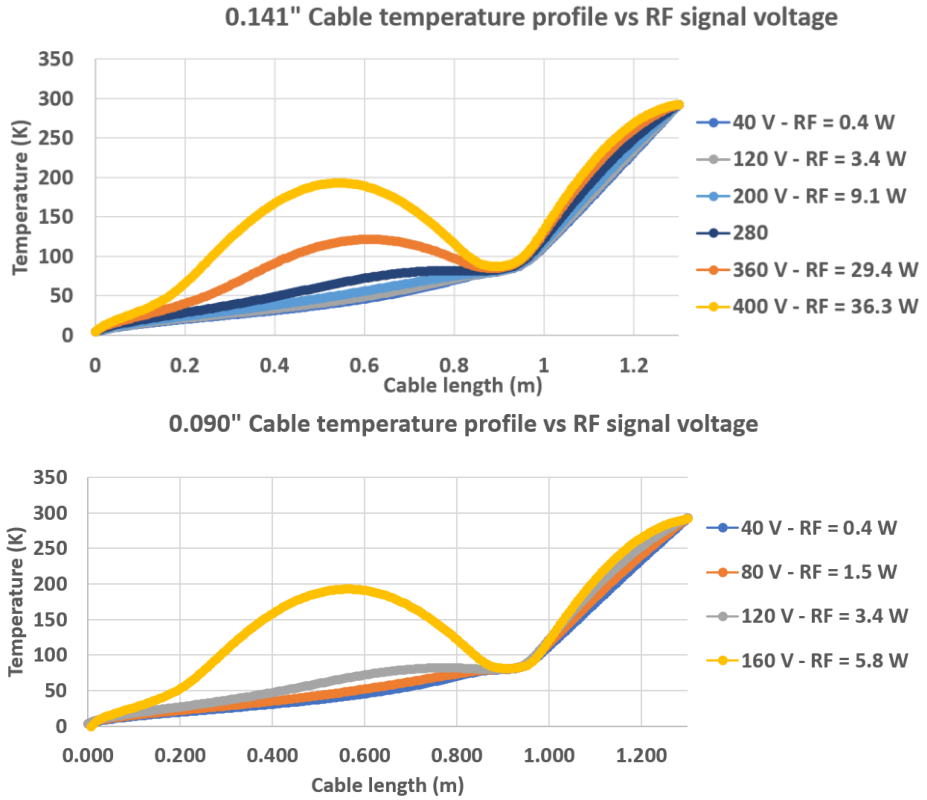

Figure 7. Temperature profile for various RF signal power for (top) 0.141" cable (bottom) 0.090" cable

As can be seen from Fig. 7, the 0.141" will produce less temperature elevation for a given RF power. Indeed, referring to Eq. (1) the bigger cable will produce less dissipated heat ($\propto \frac{1}{r_{i,e}}$) while conducting the heat away more effectively ($\propto r_{i,e}$). However, until a voltage of 160 V (RF power of 5.8 W) the use of the 0.090" cable is considered satisfactory and is not expected to produce a significant variation of its temperature profile. For comparison, the maximum voltage expected for EIC is around 80 V (RF power 1.5 W).

Although the operating temperature of the SiO_2 dielectric cable allows operating temperature well above room temperature, another issue is the differential attenuation between cables with a high heating (pickup close to the bunch) and the cables with a lower heating. Fig 8 plots the variation of cable attenuation due to the different cable temperature profile at different signal peak voltages (Fig 7).

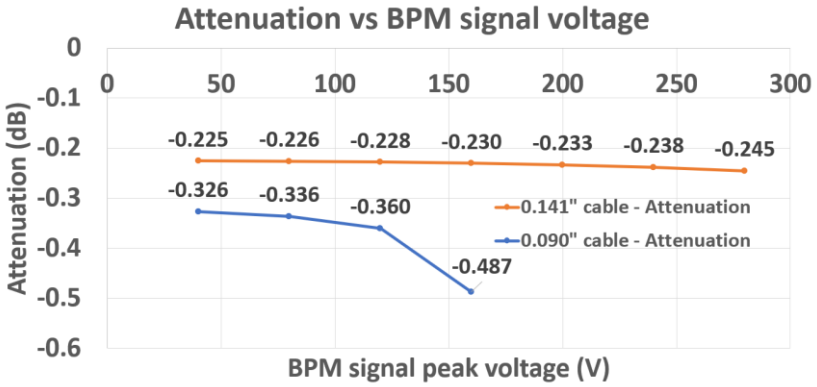

Figure 8. Signal cable attenuation for various RF signal peak voltage

A series of tests will be carried out on sample cables (like described in [4]) to validate the overall attenuation and power dissipation of the as-received RF cables.

7. Overall assembly simulation

The BPM module will be subject to heating from beam resistive wall heating, electron cloud heating, cable thermal conduction and cable and stem power dissipation. The cold sink will be the HSR beam screen cooling circuit (with temperatures ranging from 4.5 K to 9 K). As a byproduct of their electrical insulation requirement, the inner conductor and button are well insulated from the cryogenic cooling by the SiO_2 dielectric and the SiO_2 insulator spacer respectively. So heat extraction will be less easy and their heating will be more important (Fig 9). Also the electrical resistivity of pure copper will tend to increase significantly above 30 K and its thermal conductivity will show a steeper decrease. Both effect will combine and contribute to a higher resulting temperature of the pickup and cable.

Since the BPM pickup is coated with amorphous carbon coating to limit the Secondary Electron Yield (SEY), a higher level of gas cryogenically adsorbed is expected compared to bare metallic surfaces. In order to limit the release of this condensed gas with the beam heating, the temperature of the button should be contained under 40 K [10]. This is closely achieved by the current design (Fig 10). The button secondary electron could (SEY) is assumed to be 1.14 or less. Higher SEY would result in a higher heating of the button and housing [9].

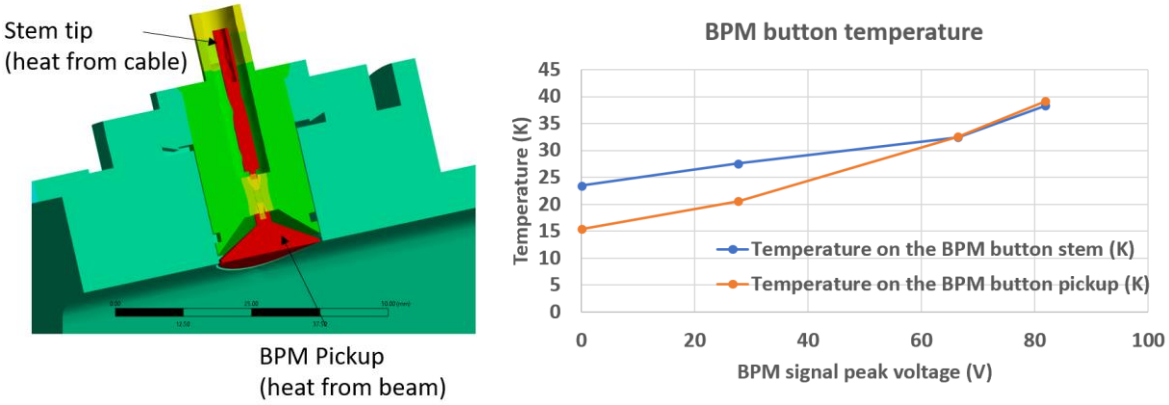

Figure 9. BPM button temperature with the 0.090" cable

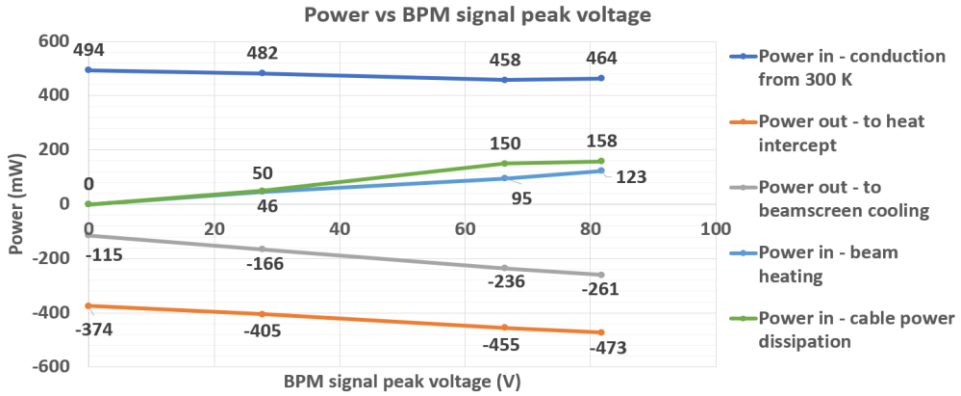

Figure 10. BPM model power with the 0.090" cable for increasing RF signal peak voltage

One way to limit the button heating will be the adoption of the smaller 0.090" SiO2 cable. Indeed, the heat conduction through the cable remains the dominant contributor to the cryogenic heat in-leak in most case simulated (Fig 10). This was confirmed by a cable heat conduction test [9].

An average gain of 0.3 W is estimated per interconnect (4x buttons) when using the smaller 0.090" cable. Summed on all HSR interconnects, the reduction in heat going to the 4.5 K side would be in the order of 75 W which equates to 24 kW of cooling power saved at the cryogenic plant (Table 2). The expected energy cost saving over the lifetime of the EIC project is significant [11].

8. Summary and outlook

An extensive engineering analysis has been made to assess the preliminary design of the HSR BPM and the final design is now underway in view of procurement. A series of tests are planned on the first SiO_2 cable to compare the actual power dissipation with the simulations for various temperatures and RF power and frequencies. If the test results are consistent with the findings described here, the thermal requirements are fulfilled, and the design is expected to operate adequately in its cryogenic environment.

9. References

[1] F Willeke and J. Beebe-Wang, "Electron Ion Collider Conceptual Design Report 2021," Feb. 2021, doi: 10.2172/1765663.

[2] S. Peggs et al., "Large Radial Shifts in the EIC Hadron Storage Ring", *Proc. IPAC'21*, Campinas, Brazil, May 2021, pp. 1443-1446, doi:10.18429/JACoW-IPAC2021-TUPAB042.

[3] M Sangroula et al."Feasability of Using the Existing RHIC Stripline BPMs for the EIC" in *Proc. IPAC'21*, Campinas, Brazil, May 2021 doi:10.18429/JACoW-IPAC2021-WEPAB194

[4] P Thieberger et al. "High intensity limitations due to signal heating of the cryogenic BPM cables" *Proc. PAC 2013* THPHO09

[5] D Gassner et al "Conceptual design overview of the Electron Ion Collider Instrumentation" in *Proc. IBIC'21 [*doi: 10.18429/JACoW-IBIC2021-MOPP04]

[6] Cameron, P., & Morvillo, M.. Thermal Behavior of RHIC BPM Cryogenic Signal Cables. United States. https://doi.org/10.2172/1119462

[7] R Than – Private conversation

[8] C Bovet et al "Measurement and modelling of the thermal dissipation of a cryogenic coaxial cable for the LHC BPMs"

[9] F Micolon et al. "Thermal simulation of the HSR arc BPM for EIC" BNL technical report BNL-224218-2023-TECH doi:10.2172/1969913

[10] R Salemme et al. "Vacuum Performance of Amorphous Carbon Coating at Cryogenic Temperature with Presence of Proton Beams", in *Proc IPAC'16* doi:10.18429/JACoW-IPAC2016-THPMY007

[11] F Micolon et al. "Estimate of the marginal cost of cryogenic heat for EIC" BNL technical report BNL-224168-2023-TECH